28 JAN. 1981

Nuclear Instruments and Methods 182-183 (1981) p. 985-990
© North-Holland Publishing Company

EFFECT OF ION IMPLANTATION ON THE OXYGEN OVERPOTENTIAL OF Ni ANODES

U. AKANO, J.A. DAVIES *, W.W. SMELTZER, I.S. TASHLYKOV ** and D.A. THOMPSON
Institute for Materials Research, McMaster University, Hamilton, Ontario, Canada L8S 4M1

This work investigates the use of ion implantation for decreasing the oxygen-overpotential of nickel anodes. It is part of a search for improved electrocatalysts to increase the energy efficiency of the H_2O electrolysis process for producing H_2 gas.

A series of Ni electrodes were implanted at room temperature with various doses of 50 keV Ag^+, Li^+, He^+, or Kr^+ ions. Polarization measurements were then made in a suitable electrolysis cell over a wide range of current densities, using aqueous KOH solution (30%) at 80°C as electrolyte. In the case of Ag^+ implants, Rutherford backscattering (RBS) measurements were performed before and after electrolysis in order to monitor the amount and depth distribution of the Ag atoms.

For Li^+ or He^+ implantation, we observe a negligible change in the measured polarization curves. For high dose Kr^+ implants (10^{18} ions cm^{-2}) the Ni electrode exhibits an increase in overpotential, indicating that excessive damage and/or sputtering of the surface causes some deterioration in electrode behaviour.

For Ag^+ implants, on the other hand, we observe a large (20–40%) reduction in the total overpotential at implant doses of $0.3–4 \times 10^{16}$ Ag^+ cm^{-2}. Furthermore, RBS measurements show that prolonged electrolysis at higher current density (24–28 h at 1 A/cm^{-2}) produces only a small loss of Ag and shifts its depth profile to significantly larger depths. Supplementary nuclear microanalyses, using the $^{16}O(d,p)^{17}O$ reaction, show that the shift in Ag profile is correlated with the growth of an anodic nickel oxide (+carbon) layer during electrolysis.

In one set of runs, the Ni electrodes were thermally oxidized before Ag^+ implantation in order to form an ~400 Å layer of NiO at the surface. In this case, we observe a somewhat smaller reduction in overpotential following Ag^+ implantation; furthermore, a large loss of Ag into the electrolyte occurs during the subsequent electrolysis.

1. Introduction

Electrolysis of water is potentially a reversible process, but electrode polarization especially at the oxygen anode increases the required voltage sufficiently to prevent the technological development of high efficiency electrolysers and fuel cells. Most commercial electrolysers and fuel cells. Most commercial electrolysers consist of Ni electrodes immersed in a hot 25–50 wt% KOH electrolyte, but they operate at relatively low voltage efficiencies. Many other metals–for example, Pt, Ru and Ag–would offer superior electrocatalytic performance to Ni, but these are generally too expensive for large scale commercial use. In this regard, ion implantation (or ion-beam-induced mixing) several potential advantages:

(i) the noble metal can be introduced into the near surface region (typically <1000 Å) to a precise and controlled concentration;

(ii) solid solubilities do not limit the maximum achievable concentration;

(iii) because only very near surface layers are being modified, the amount of noble metal can be minimized.

Several years ago, Grenness and Thompson [1] implanted Pt into tungsten and found that the electrocatalytic activity of the surface approached that of platinum itself, even though only a minute amount of platinum had been implanted. A similar study by Rabette et al., [2] examined the catalytic activity of single crystal supports of α-Al_2O_3 and MgO implanted with platinum ions. Also, in a closely related series of studies, Dearnaley [3] and others have demonstrated the value of ion implantation in producing improved corrosion resistance for various metals.

In the present investigation, we have implanted selected species (Li^+ and Ag^+) into Ni and oxidized Ni anodes and have measured the resulting change in voltage efficiency as a function of electrolysis current in a suitable H_2O-electrolysis cell. In the case of the Ag^+ implants, Rutherford backscattering (RBS) and nuclear microanalysis (NMA) have been used to monitor the Ag profile and the oxygen content of the

* Atomic Energy of Canada Limited, Chalk River, Ontario, Canada, K0J 1J0.
** Visiting Scientist from Byelorussian State Univeristy, Minsk, U.S.S.R.

РЕПОЗИТОРИЙ БГПУ

anode before and after prolonged electrolysis. Eventually, we hope to extend our investigation to include Pt implantation, but we do not yet have available the necessary ion source for producing μA beams of Pt^+. Some high-dose inert gas (He^+ and Kr^+) implants have also been studied in order to determine the possible contribution of radiation damage effects.

2. Experimental

Our 3-compartment electrolysis cell is shown in fig. 1. The main cell contains the hot (30 wt% KOH) electrolyte and the implanted Ni anode A (embedded in teflon) plus a Pt reference anode, A_{ref}; it is equipped with a cover to minimize evaporation loss.

The main *variable* electrolysis current flows between A and the platinum cathode C which is mounted in a separate compartment to minimize mixing of electrolysis products. A much smaller *constant* current of 1 mA flows between a pair of Pt reference electrodes, A_{ref} and C_{ref}, with C_{ref} also mounted in a separate compartment with only a 2 mm connecting capillary to the main cell.

We measure the potential V_1 between the nickel anode A and the Pt reference cathode C_{ref}. At the same time, we also measure the potential V_2 between C_{ref} and a reversible $Pt(H_2)$ standard electrode, R. This (dynamic cathode) potential is always quite small – i.e. ~0.040 V – and hence the observed variations in V_1 are mainly due to overvoltage effects at or near the Ni anode. Note that V_1 will include some contribution from the (iR) voltage drop in the electrolyte near the anode. However, this is not a serious complication in the present work, since our

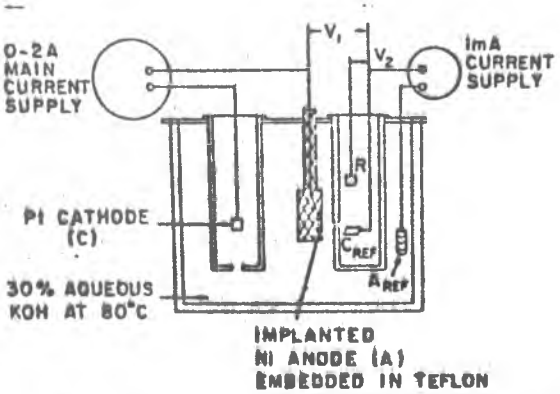

Fig. 1. Schematic diagram of the 3-compartment electrolysis cell.

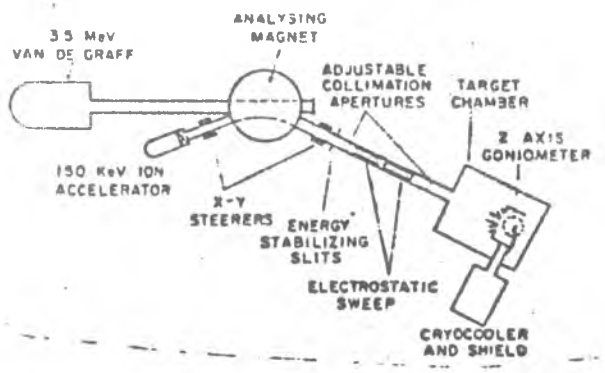

Fig. 2. Ion implantation and RBS analysis facility.

initial objective is only to identify promising implantation systems which can then be investigated more rigorously.

The Ni anodes consisted of 9 mm diameter metal discs, mechanically polished with successively finer metallurgical paper and finally with 1 μm diamond paste. After implantation, the anode was sealed into its teflon holder with a suitable epoxy in order to define reproducibly the effective surface area during electrolysis.

Fig. 2 shows schematically the ion implantation facility at McMaster. The 150 kV accelerator is used for implanting the various ions, and the 3.5 MV Van de Graaff is used for subsequent RBS analyses of the amount and depth profile of Ag^+ in the implanted electrode. Most of the Ag^+ implants and also the nuclear microanalyses were carried out at CRNL. All implants were carried out at 300 K and ~0.5 μA cm^{-2}. Note that a cryoshield at ~30 K surrounds the target in order to maintain ultra-clean vacuum conditions during both the implantation and the RBS analysis.

For the lightest ions (He^+ and Li^+), where the implant depth is quite large, each implant involved several different energies in order to obtain a relatively uniform depth distribution.

3. Results and discussion

3.1. Overpotential measurements

Table 1 summarizes the observed effects of implantation on the oxygen overpotential η of the Ni anode. Of the four implanted species studied to date, Ag^+ produced a significant reduction in η, especially

РЕПОЗИТОРИЙ БГПУ

Table 1
Electrochemical behavior of implanted Ni anodes

Implanted species	Reason for selection	Implant energy (keV)	Implant dose (ions cm^{-2})	Observed effect on η
Li^+	Li–Ni alloys give improved oxide conductivity and anode performance	15 + 40	10^{15}–10^{16}	nil
$^4He^+$	to investigate the possible influence of bombardment-induced damage or sputtering effects	15 + 40	10^{16}–10^{17}	nil
Kr^+		12	$\approx 10^{18}$	small increase
Ag^+	noble metals (Pt, Ru, etc) are known to be much better anodes than Ni	50	0.3–4.0 $\times 10^{16}$	20–40% reduction

at large values of the current density (i.e. $i \geq 0.1$ A cm^{-2})—as seen in fig. 3. The other ions all had a negligible effect on η, except Kr^+ which (at much higher dose) actually produced a small *increase* in η.

Our observed curves of η vs. current density for Ag^+-implanted anodes appear to be independent of the implant dose (table 2) over the range 0.3–1.3 × 10^{16} Ag^+ cm^{-2}, but at the highest dose used (4 × 10^{16} cm^{-2}) a somewhat larger value of η is obtained. Also, the Ag^+-implanted Ni–NiO anode shows a smaller improvement than a Ni anode with the same Ag^+ implant dose. As discussed later (fig. 6), this dif-

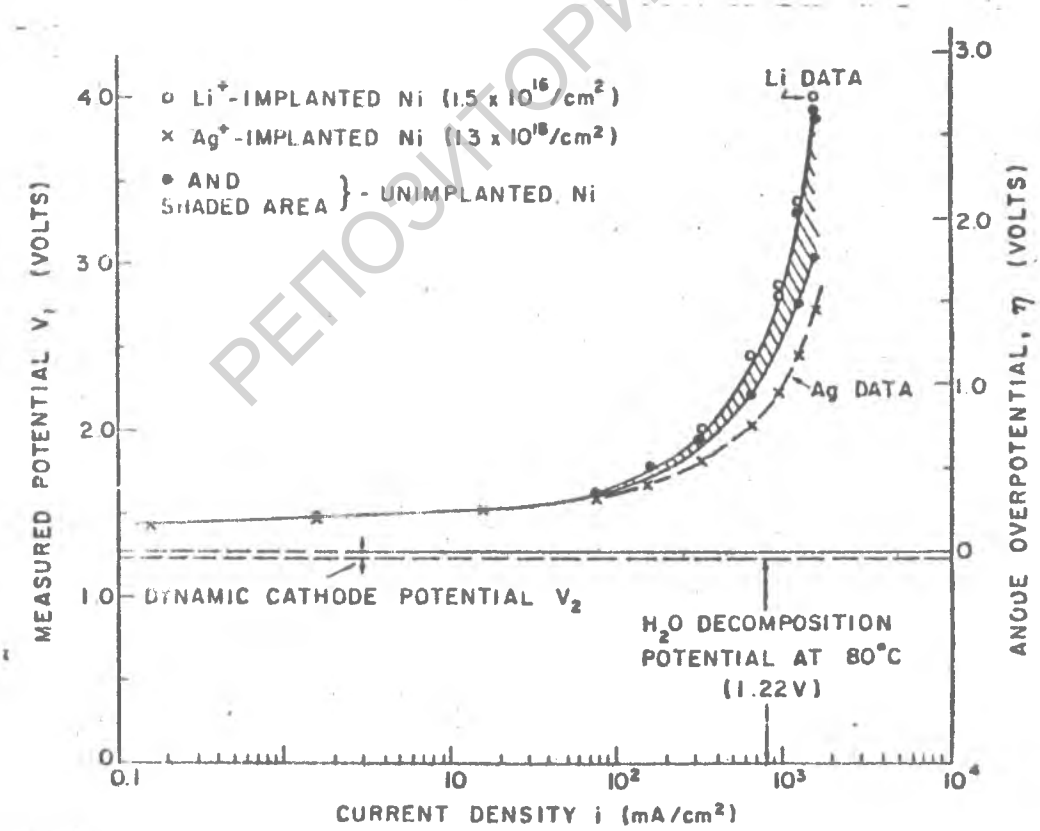

Fig. 3. Tafel plot of the observed potential V_1 vs. log i for Ag^+(+), Li^+(o) and unimplanted (shaded region) Ni anodes. The corresponding overpotential (η) values are shown on the right hand scale.

РЕПОЗИТОРИЙ БГТУ

Table 2
Overpotential η of Ag^+-implanted Ni at 1 A cm^{-2}

Target	Implant (10^{16} Ag^+ cm^{-2})	η (V)
Ni	0.3	0.94
	0.6	0.99
	1.3	0.94
	4.0	1.14
NiO	1.3	1.24
Unimplanted Ni		1.3–1.6

ference is probably associated with the large loss of Ag during electrolysis in the pre-oxidized Ni–NiO case.

One rather troublesome feature of the unimplanted Ni anodes was a rather large variation in the observed overpotential from sample to sample–as shown by the shaded area in fig. 3. The Ag^+-implanted anodes, on the other hand, gave much more reproducible η vs. log i curves. A similar but less dramatic improvement in reproducibility was also seen in the Li^+ and even in the He^+ implants. Microscopic examination of these implanted anode surfaces after prolonged electrolysis show a much more uniform corrosion film than on an unimplanted sample. Similarly, anodes which had been pre-oxidized to form an ~400 Å surface NiO layer also exhibit much better reproducibility during electrolysis than the untreated Ni anodes–and a more uniform corrosion film.

The inert gas implants (He^+ and Kr^+), at comparable doses to those used in the Ag^+ study, show no detectable change in η–indicating that radiation damage effects are not playing a significant role in the observed η reduction. Indeed, at considerably higher dose (i.e. ~10^{18} ions cm^{-2}), the Kr-implanted anodes actually exhibit a small *increase* in η.

In the case of the Li^+ implants, the lack of a significant η reduction (table 1) is somewhat surprising, since it was already known [4] that the incorporation of ~10% Li_2O into the oxidized surface of a Ni anode produces a marked increase in oxide conductivity and a consequent reduction in overpotential.

At i values $\leq$0.1 A cm^{-2}, our measured values of V_1 (and hence η) exhibit an approximately linear dependence on log i, with the slope of this Tafel plot (fig. 3) being typically ~0.05 V. At higher i values, however, V_1 increases much more rapidly and eventually approaches an almost linear dependence on i (fig. 4) indicating that the (iR) drop in the electrolyte

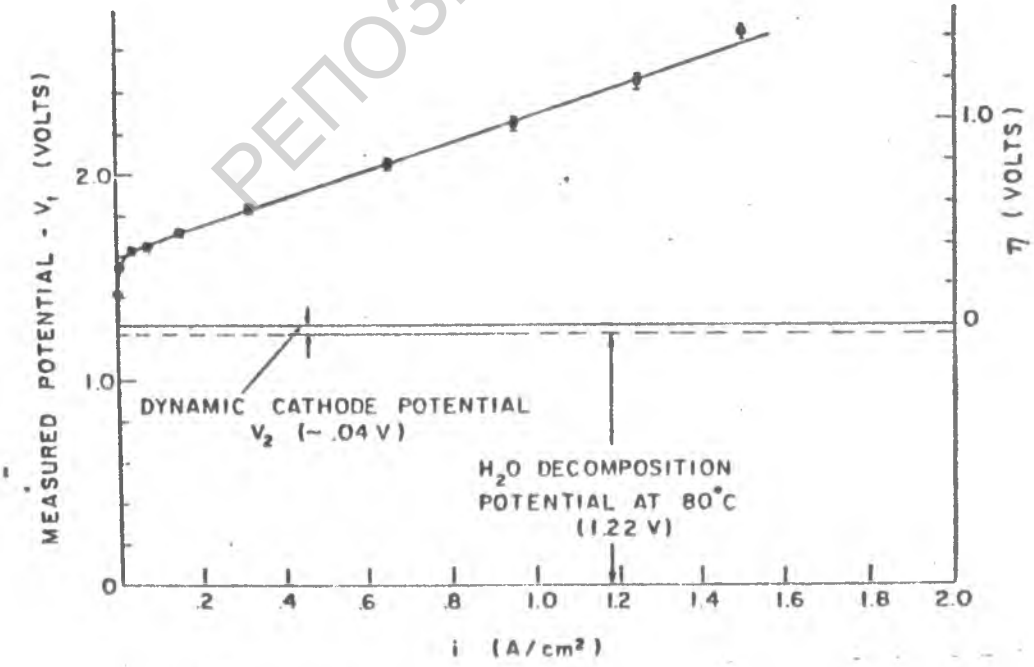

Fig. 4. Observed potential V_1 as a function of I for a Ag^+-implanted Ni anode (1.3×10^{16} Ag cm^{-2} at 50 keV).

near the anode is now starting to make a significant contribution to the V_1 measurements. Obviously, in future work, a more extensive potential-measuring technique will be required to distinguish the relative contribution of η and (iR) drop to V_1.

3.2. Anode discharge potential

After each Ni anode had been subjected to a 24 h electrolysis run, the current was turned off and the residual discharge potential was monitored for several hours. The Ag^+-implanted anodes exhibit a well-defined plateau at ~1.3 V (fig. 5) before dropping to the normal steady-state value of 0.9 V. It is interesting to note that the length of this plateau increases linearly with Ag^+ implant dose and, from the known impedance of the recording voltmeter ($1 \times 10^6\ \Omega$), we estimate that the integrated charge flowing during this plateau "phase" is equivalent roughly to two electrons per implanted Ag atom. This would suggest the formation, during electrolysis, of an intermediate complex involving the storage of ~one oxygen ion per implanted Ag atom. Note that the unimplanted Ni anode exhibits no well-defined plateau at all.

3.3. Rutherford backscattering (RBS) and nuclear microanalysis (NMA)

Before and after electrolysis, each of the Ag^+-implanted anodes was analysed by RBS, using a beam of 2.0 MeV $^4He^+$ ions. The results obtained on the 3×10^{16} atoms cm^{-2} implant are shown in fig. 6. The initial Ag peak position is seen to occur just slightly deeper than the predicted R_{LSS} implant depth. After the first 24 h electrolysis run at ~1 A cm^{-2}, the Ag peak is shifted ~200 Å deeper into the Ni, but its total area remains unchanged indicating that negligible loss of Ag has occurred.

Nuclear microanalysis, using 970 keV deuterons and the $^{16}O(d,p)^{17}O$ reaction, shows that the Ni anode had picked up $\sim 2 \times 10^{17}$ oxygen atoms cm^{-2} during this first 24 h electrolysis; this is equivalent to the formation of ~400 Å of NiO on the anode surface. Trapping of Ag at this mobile Ni–NiO interface could well explain the observed Ag peak shift in fig. 6. Simultaneous observation of the $^{12}C(d,p)^{13}C$ reaction yield shows that the surface "oxide layer" also contains a comparable number ($\sim 1.5 \times 10^{17}$ cm^{-2}) of carbon atoms and hence is more complex a molecular structure than NiO.

Further electrolyses for additional 24 h periods

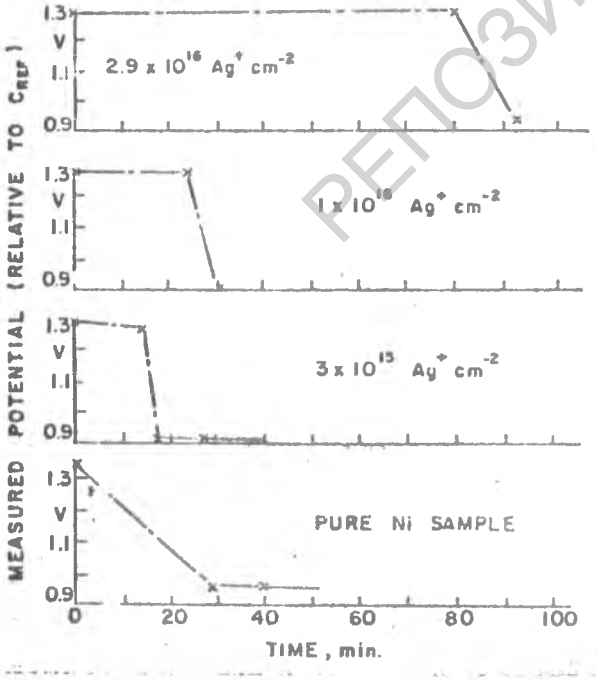

Fig. 5. Anode discharge potential (V_1) with the electrolysis current turned off.

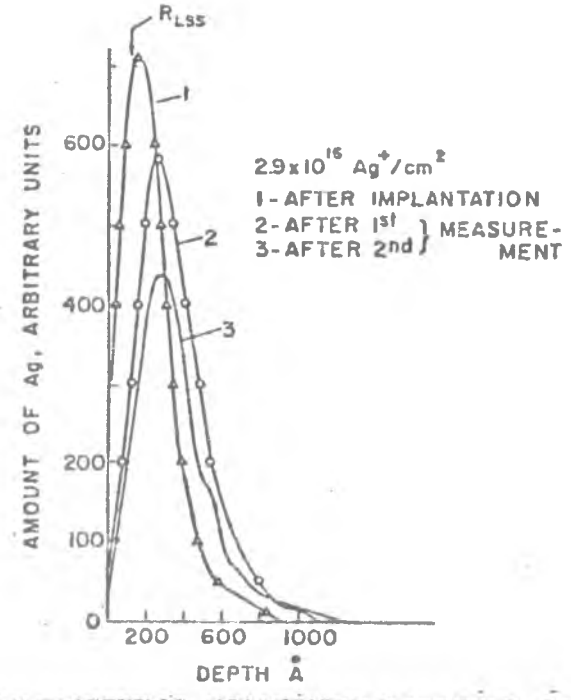

Fig. 6. RBS measurement of the implanted Ag profile in Ni before and after 24 h electrolysis runs.

РЕПОЗИТОРИЙ БГПУ

produce no further shift in the Ag peak position, but a gradual reduction in area occurs, indicating a gradual loss of Ag into the electrolyte.

A similar RBS study of Ag^+ implanted into preoxidized Ni anodes (400 Å NiO) shows no change in the Ag peak position but >50% loss to the electrolyte during the first 24 h electrolysis period. The poorer electrolytic performance of the implanted Ni–NiO anode (table 2) is probable related to this large loss of Ag into the electrolyte.

4. Conclusions

A very significant reduction in the anodic overpotential of nickel can be obtained by Ag^+ implantation at $\sim 1 \times 10^{16}$ atoms cm^{-2}, but more extensive electrochemical studies will be required to establish the relative contributions of oxygen overvoltage and electrolyte resistivity.

During electrolysis, the implanted Ag profile is swept several hundred Å deeper into the Ni, probably by trapping at the moving Ni–NiO interface.

Inert gas (He^+, Kr^+) and Li^+ implantations have negligible effect at 10^{15}–10^{16} atoms cm^{-2} implant doses.

We are especially grateful to Orville Westcott at CRNL for providing the Ag implantations.

References

[1] M. Grennes and M.W. Thompson, J. Appl. Electrochem. 4 (1974) 211.
[2] P. Rabette, A.M. Deane, A.J. Tench and M. Che, Chem. Phys. Lett. 60 (1979) 348.
[3] G. Dearnaley and N.E.W. Hartley, Thin Solid Films 54 (1978) 215; also G. Dearnaley, this proceedings.
[4] A.C.C. Tseung, B.S. Hobbs and A.D.S. Tantram, Electrochem. Acta 15 (1970) 473.

РЕПОЗИТОРИЙ БГУ